Deeksha Singh, Rajesh K. Pandey* and Martin Bohner

High-order approximation of Caputo–Prabhakar derivative with applications to linear and nonlinear fractional diffusion models

https://doi.org/10.1515/jncds-2023-0110
Received December 13, 2023; accepted August 5, 2024; published online September 2, 2024

Abstract: In this study, we devise a high-order numerical scheme to approximate the Caputo–Prabhakar derivative of order $\alpha \in (0,1)$, using an rth-order time stepping Lagrange interpolation polynomial, where $3 \leq r \in \mathbb{N}$. The devised scheme is a generalization of the existing schemes developed earlier. Further, we adopt the discussed scheme for solving a linear time fractional advection–diffusion equation and a nonlinear time fractional reaction–diffusion equation with Dirichlet type boundary conditions. We show that the discussed method is unconditionally stable, uniquely solvable and convergent with convergence order $O(\tau^{r+1-\alpha}, h^2)$, where τ and h are the temporal and spatial step sizes, respectively. Without loss of generality, applicability of the discussed method is established by illustrative examples for $r = 4, 5$.

Keywords: Caputo–Prabhakar derivative; fractional advection–diffusion equation; fractional reaction–diffusion equation; stability; convergence order

1 Introduction

Fractional calculus is one of the rapidly emerging fields due to the extensive range of applications in science and engineering, like in polymer science [1], control and signal processing [2], image processing [3], [4], physics [5] and some other applications can be seen in [6]–[8] and the references therein. One of the crucial properties of fractional operators is that they are nonlocal in nature. Due to this nonlocal behavior, finding the analytical solution of fractional differential equations is quite challenging, and this motivates us to construct an effective numerical method to solve such equations.

Various definitions of fractional derivatives and integrals and their numerical approximations are discussed in the literature [9]–[12]. In this article, we consider a fractional derivative having the three-parameter Mittag–Leffler (ML) function as its kernel. The three-parameter ML function, also called the Prabhakar function, is a generalization of the classical ML function, introduced by the Indian mathematician Tilak Raj Prabhakar in 1971 [13]. Properties and applications of the Prabhakar function have been studied by Garra et al. in [14] with a special attention to the asymptotic behavior of the function in the complex plane and on the negative semi-axis. Mainardi et al. [15] have examined local integrability and complete monotonicity of the Prabhakar function.

***Corresponding author: Rajesh K. Pandey**, Department of Mathematical Sciences, Indian Institute of Technology (BHU), Varanasi, 221005, Uttar Pradesh, India, E-mail: rkpandey.mat@iitbhu.ac.in. https://orcid.org/0000-0002-5198-4340
Deeksha Singh, Department of Mathematical Sciences, Indian Institute of Technology (BHU), Varanasi, 221005, Uttar Pradesh, India; and Department of Mathematics, College of Engineering and Technology, SRM Institute of Science and Technology, Kattankulathur 603203, Tamilnadu, India, E-mail: deekshas905@gmail.com
Martin Bohner, Department of Mathematics and Statistics, Missouri University of Science and Technology, Rolla, MO, USA, E-mail: bohner@mst.edu

Srivastava et al. [16] established some new connections between the ML functions of one, two, and three parameters and expressed the three-parameter ML function as a fractional derivative of the two-parameter ML function. The numerical evaluation of the Prabhakar function was studied by Garrappa in [17], and he also developed a Matlab code to calculate the Prabhakar function numerically [18]. For a more detailed study of the Prabhakar function and derivatives and integrals involving the Prabhakar function, we refer the readers to [19], [20] and the references therein.

In this work, we consider the Caputo–Prabhakar fractional derivative, which is a generalization of the Caputo derivative obtained by introducing the Prabhakar function in the kernel as

$$ {}_0^{CP}D^{\gamma}_{\rho,\alpha,\omega} f(t) = \int_0^t (t-s)^{-\alpha} E^{-\gamma}_{\rho,1-\alpha}(\omega(t-s)^{\rho}) f'(s)\mathrm{d}s, \tag{1} $$

where $0 < \alpha < 1$ is the order of the derivative and $E^{\gamma}_{\alpha,\beta}(\zeta) = \sum_{m=0}^{\infty} \frac{\Gamma(\gamma+m)\zeta^m}{\Gamma(\gamma)\Gamma(\alpha m+\beta)m!}$ is the three-parameter ML function, such that $\alpha, \beta, \gamma, \zeta \in \mathbb{C}$ and $\mathrm{Re}(\alpha) > 0$.

Applications of Prabhakar fractional derivatives are found in fractional viscoelasticity [21], anomalous dielectrics [22], and anomalous relaxation models [23]. Numerical approximation of Caputo–Prabhakar derivatives has been used to find approximate solution of fractional-order integro-differential equations using different approaches such as Legendre wavelet method [24], Haar wavelet collocation method [25], and Chebyshev polynomials [26]. Derakhshan et al. studied numerical approximation of fractional Sturm–Liouville problems using Caputo–Prabhakar derivatives [27].

Numerous studies have been done on numerical solutions of fractional-order differential equations with Caputo–Prabhakar derivative. For example, Eshaghi et al. studied a fractional Black–Scholes model [28] and stability and dynamics of neutral and integro differential systems of fractional order [29], Derakhshan et al. gave a comparison between homotopy perturbation transform and fractional Adams–Bashforth method for the solution of nonlinear fractional differential equations [30], Garrappa et al. studied stability of fractional-order systems with Caputo–Prabhakar derivative [31]. In our previous work [32], we have used Lagrange interpolation polynomials of degrees one and two for numerical approximation of the Caputo–Prabhakar derivative of order $0 < \alpha < 1$, with convergence orders $(2-\alpha)$ and $(3-\alpha)$, respectively, and used this approximation to solve time fractional advection–diffusion equations. Various numerical methods are available for numerical approximation of fractional advection–diffusion equation [33]–[38]. However, papers available for the numerical approximation of fractional-order systems involving Prabhakar fractional derivative are very few, which prompted us to study an efficient numerical scheme for approximation of Caputo–Prabhakar derivatives.

So, in this article, we develop a high-order numerical scheme using an rth-order Lagrange interpolation polynomial for the approximation of the Caputo–Prabhakar derivative (1), which is motivated by the work of Li et al. [39]. Further, we use this approximation to solve linear and nonlinear time fractional models namely, time fractional advection–diffusion equation and time fractional reaction–diffusion equation with Dirichlet type boundary conditions using central difference approximation in space. The nonlinear reaction term in reaction–diffusion equation is approximated using the Newton–Raphson iterative method. The order of convergence of the whole discretized scheme is $O(\tau^{r+1-\alpha}, h^2)$, where τ and h denote the temporal and spatial step sizes, respectively. The stability analysis of the finite difference scheme is discussed using von Neumann stability analysis. Further, we studied the solvability and convergence analysis of the scheme. In terms of test examples, we have shown that the numerical results validate our analytical conclusions, and the scheme works well. As far as we know, no work has yet been done for the high-order approximation of Caputo–Prabhakar derivatives as discussed in this paper.

The outline of the paper is as follows: Section 2 is devoted to the study of the numerical method for approximation of the Caputo–Prabhakar derivative and discusses some properties of the discretization coefficients. Further, the error analysis of the scheme is discussed. In Section 3, we use the discussed numerical scheme to solve the time-fractional advection–diffusion equation and study stability analysis of the scheme using the von Neumann stability analysis method. This section further deals with the solvability and convergence analysis

of the numerical method. In Section 4, another application of the discussed numerical scheme in solving time fractional nonlinear reaction–diffusion equations is studied. Further, stability and convergence analysis of the scheme are discussed in Subsections 4.1, 4.2. In Subsections 2.2, 3.4, 4.3, some numerical illustrations are given to ensure the validity of our schemes. The last section offers some conclusions.

2 Numerical scheme

In this section, we develop a high-order numerical scheme to approximate (1) using time stepping Lagrange interpolation polynomials of degree r, motivated by the research work done in [32], [39]. Let $f \in C^r[0,T]$, we choose a partition, $0 = t_0 < t_1 < \ldots < t_M = T,\ M \in \mathbb{N}$, of the temporal domain $[0,T]$, with uniform step size $\tau = \frac{T}{M}$ such that $t_k = k\tau$, for $k = 0, \ldots, M$. At node $t = t_k$,

$$\begin{aligned} {}_0^{CP}D^{\gamma}_{\rho,\alpha,\omega} f(t_k) &= \int_0^{t_k} (t_k - s)^{-\alpha} E^{-\gamma}_{\rho,1-\alpha}(\omega(t_k - s)^{\rho}) f'(s)\mathrm{d}s \\ &= \sum_{j=1}^{k} \int_{t_{j-1}}^{t_j} (t_k - s)^{-\alpha} E^{-\gamma}_{\rho,1-\alpha}(\omega(t_k - s)^{\rho}) f'(s)\mathrm{d}s \\ &= \sum_{j=1}^{k} I_j[f(s)], \end{aligned} \tag{2}$$

where

$$I_j[f(s)] = \int_{t_{j-1}}^{t_j} (t_k - s)^{-\alpha} E^{-\gamma}_{\rho,1-\alpha}(\omega(t_k - s)^{\rho}) f'(s)\mathrm{d}s. \tag{3}$$

Now we discuss two separate cases for the subinterval $[t_{j-1}, t_j]$.

Case (1): For $k \geq j \geq r, M \geq k \geq r$.

The rth-order Lagrange interpolation polynomial approximating a function f at the nodes $(t_j, f(t_j))$, $(t_{j-1}, f(t_{j-1}))$, …, $(t_{j-r}, f(t_{j-r}))$ is defined as

$$p_r(t) = \sum_{i=0}^{r} f(t_{j-i}) \prod_{\substack{l=0 \\ l\neq i}}^{r} \frac{t - t_{j-l}}{t_{j-i} - t_{j-l}}, \qquad t \in [t_{j-1}, t_j],$$

and the error involved in approximating $f(t)$ by the interpolating polynomial $p_r(t)$ is

$$f(t) - p_r(t) = \frac{f^{(r+1)}(\xi_j)}{(r+1)!} \prod_{l=0}^{r} (t - t_{j-l}), \qquad \xi_j \in (t_{j-r}, t_j). \tag{4}$$

Also, we obtain

$$p_r'(t) = \sum_{i=0}^{r} f(t_{j-i}) \frac{(-1)^i}{i!(r-i)!\tau^r} \frac{d}{\mathrm{d}t} \prod_{\substack{l=0 \\ l\neq i}}^{r} (t - t_{j-l}). \tag{5}$$

Approximating $f(s)$ by $p_r(s)$ in (3), we obtain

$$I_j[f(s)] \approx I_j[p_r(s)] = \int_{t_{j-1}}^{t_j} (t_k - s)^{-\alpha} E^{-\gamma}_{\rho,1-\alpha}(\omega(t_k - s)^{\rho}) p_r'(s)\mathrm{d}s$$

$$= \int_{t_{j-1}}^{t_j} (t_k - s)^{-\alpha} E^{-\gamma}_{\rho,1-\alpha}(\omega(t_k - s)^{\rho}) \sum_{i=0}^{r} f(t_{j-i}) \frac{(-1)^i}{i!(r-i)!\tau^r} \frac{d}{ds} \prod_{\substack{l=0 \\ l\neq i}}^{r} (s - t_{j-l}) ds$$

$$= \sum_{i=0}^{r} \frac{(-1)^i}{i!(r-i)!\tau^r} f(t_{j-i}) \int_{t_{j-1}}^{t_j} (t_k - s)^{-\alpha} E^{-\gamma}_{\rho,1-\alpha}(\omega(t_k - s)^{\rho}) \frac{d}{ds} \prod_{\substack{l=0 \\ l\neq i}}^{r} (s - t_{j-l}) ds$$

$$= \tau^{-\alpha} \sum_{i=0}^{r} W^r_{i,k-j} f(t_{j-i}),$$

where

$$W^r_{i,k-j} = \frac{(-1)^{i+1}}{i!(r-i)!} \sum_{n=1}^{r} n! \left(\theta^{r-n}_{r+1,i} \phi^{k-j}_n - \lambda^{r-n}_{r+1,i} \psi^{k-j}_n \right), \quad 0 \le i \le r,$$

$$\phi^{k-j}_n = (k-j)^{n-\alpha} E^{-\gamma}_{\rho,n+1-\alpha}\left(\omega((k-j)\tau)^{\rho}\right),$$

$$\psi^{k-j}_n = (k-j+1)^{n-\alpha} E^{-\gamma}_{\rho,n+1-\alpha}\left(\omega((k-j+1)\tau)^{\rho}\right),$$

$$\theta^l_{j,i} = \begin{cases} a^l_{j,i}, & l \neq 0 \\ 1, & l = 0, \end{cases} \qquad \lambda^l_{j,i} = \begin{cases} b^l_{j,i}, & l \neq 0 \\ 1, & l = 0. \end{cases}$$

Here, $a^l_{j,i}$ is obtained from the set $X_{j,i} = ([0, j-1]\backslash\{i\}) \cap \mathbb{Z}$, and $b^l_{j,i}$ is obtained from the set $Y_{j,i} = ([-1, j-2]\backslash\{i-1\}) \cap \mathbb{Z}$, by summing the products of different possible combinations of l elements.

Now, the values of the weight coefficients $W^r_{i,k-j}$ for different $r = 1, 2, 3, 4, 5$ can be obtained as follows.

For $r = 1$,

$$\begin{cases} W^1_{0,z} = -\left[\phi^z_1 - \psi^z_1\right], \\ W^1_{1,z} = \left[\phi^z_1 - \psi^z_1\right]. \end{cases}$$

For $r = 2$,

$$\begin{cases} W^2_{0,z} = -\frac{1}{2}\left[\left(3\phi^z_1 - \psi^z_1\right) + 2\left(\phi^z_2 - \psi^z_2\right)\right], \\ W^2_{1,z} = \left[\left(2\phi^z_1\right) + 2\left(\phi^z_2 - \psi^z_2\right)\right], \\ W^2_{2,z} = -\frac{1}{2}\left[\left(\phi^z_1 + \psi^z_1\right) + 2\left(\phi^z_2 - \psi^z_2\right)\right]. \end{cases}$$

For $r = 3$,

$$\begin{cases} W^3_{0,z} = -\frac{1}{6}\left[\left(11\phi^z_1 - 2\psi^z_1\right) + 2\left(6\phi^z_2 - 3\psi^z_2\right) + 6\left(\phi^z_3 - \psi^z_3\right)\right], \\ W^3_{1,z} = \frac{1}{2}\left[\left(6\phi^z_1 + \psi^z_1\right) + 2\left(5\phi^z_2 - 2\psi^z_2\right) + 6\left(\phi^z_3 - \psi^z_3\right)\right], \\ W^3_{2,z} = -\frac{1}{2}\left[\left(3\phi^z_1 + 2\psi^z_1\right) + 2\left(4\phi^z_2 - \psi^z_2\right) + 6\left(\phi^z_3 - \psi^z_3\right)\right], \\ W^3_{3,z} = \frac{1}{6}\left[\left(2\phi^z_1 + \psi^z_1\right) + 2\left(3\phi^z_2\right) + 6\left(\phi^z_3 - \psi^z_3\right)\right]. \end{cases}$$

For $r = 4$,

$$\begin{cases} W_{0,z}^4 = -\frac{1}{24}\left[\left(50\phi_1^z - 6\psi_1^z\right) + 2\left(35\phi_2^z - 11\psi_2^z\right) + 6\left(10\phi_3^z - 6\psi_3^z\right) + 24\left(\phi_4^z - \psi_4^z\right)\right], \\ W_{1,z}^4 = \frac{1}{6}\left[\left(24\phi_1^z + 5\psi_1^z\right) + 2\left(26\phi_2^z - 5\psi_2^z\right) + 6\left(9\phi_3^z - 5\psi_3^z\right) + 24\left(\phi_4^z - \psi_4^z\right)\right], \\ W_{2,z}^4 = -\frac{1}{4}\left[\left(12\phi_1^z + 6\psi_1^z\right) + 2\left(19\phi_2^z - \psi_2^z\right) + 6\left(8\phi_3^z - 4\psi_3^z\right) + 24\left(\phi_4^z - \psi_4^z\right)\right], \\ W_{3,z}^4 = \frac{1}{6}\left[\left(8\phi_1^z + 3\psi_1^z\right) + 2\left(14\phi_2^z + \psi_2^z\right) + 6\left(7\phi_3^z - 3\psi_3^z\right) + 24\left(\phi_4^z - \psi_4^z\right)\right], \\ W_{4,z}^4 = -\frac{1}{24}\left[\left(6\phi_1^z + 2\psi_1^z\right) + 2\left(11\phi_2^z + \psi_2^z\right) + 6\left(6\phi_3^z - 2\psi_3^z\right) + 24\left(\phi_4^z - \psi_4^z\right)\right]. \end{cases}$$

For $r = 5$,

$$\begin{cases} W_{0,z}^5 = -\frac{1}{120}\left[\left(274\phi_1^z - 24\psi_1^z\right) + 2\left(225\phi_2^z - 50\psi_2^z\right) + 6\left(85\phi_3^z - 35\psi_3^z\right) + 24\left(15\phi_4^z - 10\psi_4^z\right) + 120\left(\phi_5^z - \psi_5^z\right)\right], \\ W_{1,z}^5 = \frac{1}{24}\left[\left(120\phi_1^z + 26\psi_1^z\right) + 2\left(154\phi_2^z - 15\psi_2^z\right) + 6\left(71\phi_3^z - 25\psi_3^z\right) + 24\left(14\phi_4^z - 9\psi_4^z\right) + 120\left(\phi_5^z - \psi_5^z\right)\right], \\ W_{2,z}^5 = -\frac{1}{12}\left[\left(60\phi_1^z + 24\psi_1^z\right) + 2\left(107\phi_2^z + 2\psi_2^z\right) + 6\left(59\phi_3^z - 17\psi_3^z\right) + 24\left(13\phi_4^z - 8\psi_4^z\right) + 120\left(\phi_5^z - \psi_5^z\right)\right], \\ W_{3,z}^5 = \frac{1}{12}\left[\left(40\phi_1^z + 12\psi_1^z\right) + 2\left(78\phi_2^z + 7\psi_2^z\right) + 6\left(49\phi_3^z - 11\psi_3^z\right) + 24\left(12\phi_4^z - 7\psi_4^z\right) + 120\left(\phi_5^z - \psi_5^z\right)\right], \\ W_{4,z}^5 = -\frac{1}{24}\left[\left(30\phi_1^z + 8\psi_1^z\right) + 2\left(61\phi_2^z + 6\psi_2^z\right) + 6\left(41\phi_3^z - 7\psi_3^z\right) + 24\left(11\phi_4^z - 6\psi_4^z\right) + 120\left(\phi_5^z - \psi_5^z\right)\right], \\ W_{5,z}^5 = \frac{1}{120}\left[\left(24\phi_1^z + 6\psi_1^z\right) + 2\left(50\phi_2^z + 5\psi_2^z\right) + 6\left(35\phi_3^z - 5\psi_3^z\right) + 24\left(10\phi_4^z - 5\psi_4^z\right) + 120\left(\phi_5^z - \psi_5^z\right)\right]. \end{cases}$$

Case (2): $1 \le j \le k, 1 \le k \le r-1$.

In this case, since $j < r$, we do not have sufficient points to construct the Lagrange interpolating polynomial of degree r. Hence, for each $0 < j < r$, $I_j[f(s)]$ is approximated by $I_j[P_j(s)]$, where $P_j(s)$ is a Lagrange interpolation polynomial of degree j.

Now, combining Cases (1) and (2), a numerical scheme approximating the Caputo–Prabhakar derivative is obtained as

$$\begin{aligned} {}_0^{CP}D_{\rho,\alpha,\omega}^{\gamma} f(t_k) &= \sum_{j=1}^{k} I_j[f(s)] \\ &= \sum_{j=1}^{r-1} I_j[P_j(s)] + \sum_{j=r}^{k} I_j[P_r(s)] \\ &= \tau^{-\alpha} \sum_{j=1}^{r-1} \sum_{i=0}^{j} W_{i,k-j}^{j} f(t_{j-i}) + \tau^{-\alpha} \sum_{j=r}^{k} \sum_{i=0}^{r} W_{i,k-j}^{r} f(t_{j-i}) \\ &= \tau^{-\alpha} I_k A_{k,r} f_k = \tau^{-\alpha} P_k^r f_k \\ &= \tau^{-\alpha} \sum_{j=0}^{k} p_{k-j}^r f_j + E_r^k, \end{aligned} \tag{6}$$

where

$$P_k^r = \left(p_k^r, p_{k-1}^r, \ldots, p_0^r\right) = I_k A_{k,r},$$

$$I_k = \begin{bmatrix} 1 & 1 & \ldots & 1 \end{bmatrix}_{1\times k}, \quad f_k = \left[f(t_0), \ldots, f(t_k)\right]^T,$$

$$A_{k,r} = \begin{bmatrix} W_{k,r-1} & \mathbf{0} \\ W_{k,r}^* & \end{bmatrix}_{k\times(k+1)},$$

$$W_{k,s} = \begin{bmatrix} W^1_{1,k-1} & W^1_{0,k-1} & 0 & \cdots & 0 \\ W^2_{2,k-2} & W^2_{1,k-2} & W^2_{0,k-2} & \ddots & \vdots \\ \vdots & \vdots & \vdots & \ddots & 0 \\ W^s_{s,k-s} & \cdots & \cdots & \cdots & W^s_{0,k-s} \end{bmatrix}_{s\times(s+1)},$$

$$W^*_{k,r} = \begin{bmatrix} W^r_{r,k-r} & \cdots & \cdots & \cdots & W^r_{0,k-r} & 0 & \cdots & 0 \\ 0 & W^r_{r,k-r-1} & \cdots & \cdots & \cdots & W^r_{0,k-r-1} & \ddots & \vdots \\ \vdots & \ddots & \ddots & & & & \ddots & 0 \\ 0 & \cdots & 0 & W^r_{r,0} & \cdots & \cdots & \cdots & W^r_{0,0} \end{bmatrix}_{(k-r+1)\times(k+1)}.$$

Remark 1. If $k < r$, then we can write the derived scheme as

$$ {}_0^{CP}D^{\gamma}_{\rho,\alpha,\omega} f(t_k) = \sum_{j=1}^{k} I_j[f(s)] + E^k_r. \tag{7}$$

Also when $1 \le k < r$, then $A_{k,r} = W_{k,k}$.

Next, some properties of the discretization coefficients p^r_{k-j} will be studied for $r = 4$. For other values of $4 < r \in \mathbb{N}$, it can be studied in a similar way, so those calculations are omitted.

Lemma 1. *The following relations hold between the discretization coefficients:*

1. *If we fix $k = 1$, then $p^r_1 = -p^r_0$.*
2. $\sum_{j=0}^{k} p^r_{k-j} = 0.$

Proof

1. Fixing $k = 1$, the numerical scheme (6) reduces to (7), so we have

$$p^r_1 = W^1_{1,0} = \phi^0_1 - \psi^0_1,$$

$$p^r_0 = W^1_{0,0} = -\left[\phi^0_1 - \psi^0_1\right],$$

and hence, $p^r_1 = -p^r_0$.

2. For $k = 1$,

$$\sum_{j=0}^{k} p^r_{k-j} = W^1_{0,0} + W^1_{1,0} = 0.$$

For $k = 2$,

$$\begin{aligned} \sum_{j=0}^{k} p^r_{k-j} &= W^1_{1,1} + W^2_{2,0} + W^1_{0,1} + W^2_{1,0} + W^2_{0,0} \\ &= \left(W^1_{0,1} + W^1_{1,1}\right) + \left(W^2_{0,0} + W^2_{1,0} + W^2_{2,0}\right) \\ &= 0. \end{aligned}$$

For $k = 3$,

$$\sum_{j=0}^{k} p^r_{k-j} = W^1_{1,2} + W^2_{2,1} + W^3_{3,0} + W^1_{0,2} + W^2_{1,1} + W^3_{2,0} + W^2_{0,1} + W^3_{1,0} + W^3_{0,0}$$

$$= \left(W_{0,2}^1 + W_{1,2}^1\right) + \left(W_{0,1}^2 + W_{1,1}^2 + W_{2,1}^2\right) + \left(W_{0,0}^3 + W_{1,0}^3 + W_{2,0}^3 + W_{3,0}^3\right)$$
$$= 0.$$

For $k \geq 4$,

$$\begin{aligned}\sum_{j=0}^{k} p_{k-j}^r &= \left(W_{0,k-1}^1 + W_{1,k-1}^1\right) + \left(W_{0,k-2}^2 + W_{1,k-2}^2 + W_{2,k-2}^2\right) \\ &\quad + \left(W_{0,k-3}^3 + W_{1,k-3}^3 + W_{2,k-3}^3 + W_{3,k-3}^3\right) \\ &\quad + \left(W_{0,k-4}^4 + W_{1,k-4}^4 + W_{2,k-4}^4 + W_{3,k-4}^4 + W_{4,k-4}^4\right) \\ &\quad + \left(W_{0,k-5}^4 + W_{1,k-5}^4 + W_{2,k-5}^4 + W_{3,k-5}^4 + W_{4,k-5}^4\right) \\ &\quad + \cdots + \left(W_{0,0}^4 + W_{1,0}^4 + W_{2,0}^4 + W_{3,0}^4 + W_{4,0}^4\right) \\ &= 0.\end{aligned}$$

This completes the proof. □

2.1 Error analysis of the scheme

Theorem 1. *If $f \in C^r[0,T]$, where $3 \leq r \in \mathbb{N}$, then for $\alpha \in (0,1)$, the local truncation error E_r^k satisfies the relation*

1. $\left|E_r^1\right| \leq C_1 \max_{t_0 \leq t \leq t_1} \left|f''(t)\right| \tau^{2-\alpha},\ k = 1,$
2. $\left|E_r^2\right| \leq C_2 \max_{t_0 \leq t \leq t_2} \left|f'''(t)\right| \tau^{3-\alpha},\ k = 2,$
3. $\left|E_r^k\right| \leq C_3 \max_{t_0 \leq t \leq t_k} \left|f^{(k+1)}(t)\right| \tau^{k+1-\alpha},\ 2 < k < r,\ f^{(i)}(0) = 0, 0 < i \leq k-1,$
4. $\left|E_r^k\right| \leq C_4 \max_{t_0 \leq t \leq t_n} \left|f^{(k+1)}(t)\right| \tau^{r+1-\alpha},\ k \geq r,\ f^{(i)}(0) = 0,\ 0 < i \leq r-1,$

where C_1, C_2, C_3 and C_4 are positive constants.

Proof

1. For $k = 1$, the scheme (6) is obtained by using an interpolating polynomial of degree one, and its order of convergence is $(2-\alpha)$ [32].
2. For $k = 2$, the scheme (6) is obtained by using an interpolating polynomial of degree two, and its order of convergence is $(3-\alpha)$ [32].
3. For $2 < k < r$,

$$\begin{aligned}\left|E_r^k\right| &= \left|\sum_{j=1}^{k-1} \int_{t_{j-1}}^{t_j} (t_k - s)^{-\alpha} E_{\rho,1-\alpha}^{-\gamma}(\omega(t_k - s)^\rho)(f - p_j)'(s)\mathrm{d}s \right. \\ &\quad \left. + \int_{t_{k-1}}^{t_k} (t_k - s)^{-\alpha} E_{\rho,1-\alpha}^{-\gamma}(\omega(t_k - s)^\rho)(f - p_k)'(s)\mathrm{d}s \right| \\ &= \left|\sum_{j=1}^{k-1} \int_{t_{j-1}}^{t_j} (t_k - s)^{-\alpha-1} E_{\rho,-\alpha}^{-\gamma}(\omega(t_k - s)^\rho)(f(s) - p_j(s))\mathrm{d}s\right.\end{aligned}$$

$$+\int_{t_{k-1}}^{t_k}(t_k-s)^{-\alpha-1}E^{-\gamma}_{\rho,-\alpha}(\omega(t_k-s)^{\rho})(f(s)-p_k(s))\mathrm{d}s\Bigg|.$$

Now, we consider the first integral:

$$\begin{aligned}
&\sum_{j=1}^{k-1}\int_{t_{j-1}}^{t_j}(t_k-s)^{-\alpha-1}E^{-\gamma}_{\rho,-\alpha}(\omega(t_k-s)^{\rho})(f(s)-p_j(s))\mathrm{d}s\\
&=\sum_{j=1}^{k-1}\frac{f^{(j+1)}(\xi_j)}{(j+1)!}\int_{t_{j-1}}^{t_j}(s-t_j)(s-t_{j-1})\dots(s-t_0)(t_k-s)^{-\alpha-1}E^{-\gamma}_{\rho,-\alpha}(\omega(t_k-s)^{\rho})\mathrm{d}s\\
&\le\sum_{j=1}^{k-1}-\frac{f^{(j+1)}(\xi_j)}{(j+1)}\frac{\tau^{j+1}}{4}\int_{t_{j-1}}^{t_j}(t_k-s)^{-\alpha-1}E^{-\gamma}_{\rho,-\alpha}(\omega(t_k-s)^{\rho})\\
&\le\sum_{j=1}^{k-1}-\frac{f^{(j+1)}(\xi_j)}{4(j+1)}\tau^{j+1-\alpha}\Big[(k-j)^{-\alpha}E^{-\gamma}_{\rho,1-\alpha}(\omega(t_k-t_j)^{\rho})\\
&\quad-(k-j+1)^{-\alpha}E^{-\gamma}_{\rho,1-\alpha}(\omega(t_k-t_{j-1})^{\rho})\Big].
\end{aligned}\tag{8}$$

Next, we consider the second interval:

$$\begin{aligned}
&\int_{t_{k-1}}^{t_k}(t_k-s)^{-\alpha-1}E^{-\gamma}_{\rho,-\alpha}(\omega(t_k-s)^{\rho})(f(s)-P_k(s))\mathrm{d}s\\
&=\int_{t_{k-1}}^{t_k}\frac{f^{(k+1)}(\xi)}{(k+1)!}(s-t_0)(s-t_1)\dots(s-t_k)(t_k-s)^{-\alpha-1}E^{-\gamma}_{\rho,-\alpha}(\omega(t_k-s)^{\rho})\mathrm{d}s\\
&\le-\frac{f^{(k+1)}(\xi)}{4(k+1)}\tau^{k+1}\int_{t_{k-1}}^{t_k}(t_k-s)^{-\alpha-1}E^{-\gamma}_{\rho,-\alpha}(\omega(t_k-s)^{\rho})\mathrm{d}s\\
&=-\frac{f^{(k+1)}(\xi)}{4(k+1)}\tau^{k+1-\alpha}E^{-\gamma}_{\rho,1-\alpha}(\omega\tau^{\rho}).
\end{aligned}\tag{9}$$

Now, combining (8) and (9), we have

$$\begin{aligned}
\left|E_r^k\right|&\le\Bigg|\sum_{j=1}^{k-1}\frac{f^{(j+1)}(\xi_j)}{4(j+1)}\tau^{j+1-\alpha}\Big[(k-j)^{-\alpha}E^{-\gamma}_{\rho,1-\alpha}(\omega(t_k-t_j)^{\rho})\\
&\quad-(k-j+1)^{-\alpha}E^{-\gamma}_{\rho,1-\alpha}(\omega(t_k-t_{j-1})^{\rho})\Big]\\
&\quad+\frac{f^{(k+1)}(\xi)}{4(k+1)}\tau^{k+1-\alpha}E^{-\gamma}_{\rho,1-\alpha}(\omega\tau^{\rho})\Bigg|\\
&\le C_3\max_{t_0\le t\le t_k}\left|f^{(k+1)}(t)\right|\tau^{k+1-\alpha},
\end{aligned}$$

where C_3 is a positive constant.

4. For $k \geq r$,

$$\begin{aligned}
\left|E_r^k\right| &= \left|\sum_{j=1}^{r-1}\int_{t_{j-1}}^{t_j}(t_k-s)^{-\alpha}E_{\rho,1-\alpha}^{-\gamma}(\omega(t_k-s)^{\rho})(f-P_j)'(s)\mathrm{d}s\right.\\
&\quad+\sum_{j=r}^{k-1}\int_{t_{j-1}}^{t_j}(t_k-s)^{-\alpha}E_{\rho,1-\alpha}^{-\gamma}(\omega(t_k-s)^{\rho})(f-P_r)'(s)\mathrm{d}s\\
&\quad\left.+\int_{t_{k-1}}^{t_k}(t_k-s)^{-\alpha}E_{\rho,1-\alpha}^{-\gamma}(\omega(t_k-s)^{\rho})(f-P_r)'(s)\mathrm{d}s\right|\\
&=\left|\sum_{j=1}^{r-1}\int_{t_{j-1}}^{t_j}(t_k-s)^{-\alpha-1}E_{\rho,-\alpha}^{-\gamma}(\omega(t_k-s)^{\rho})(f(s)-P_j(s))\mathrm{d}s\right.\\
&\quad+\sum_{j=r}^{k-1}\int_{t_{j-1}}^{t_j}(t_k-s)^{-\alpha-1}E_{\rho,-\alpha}^{-\gamma}(\omega(t_k-s)^{\rho})(f(s)-P_r(s))\mathrm{d}s\\
&\quad\left.+\int_{t_{k-1}}^{t_k}(t_k-s)^{-\alpha-1}E_{\rho,-\alpha}^{-\gamma}(\omega(t_k-s)^{\rho})(f(s)-P_r(s))\mathrm{d}s\right|.
\end{aligned}$$

We will consider the first integral:

$$\begin{aligned}
&\sum_{j=1}^{r-1}\int_{t_{j-1}}^{t_j}(t_k-s)^{-\alpha-1}E_{\rho,-\alpha}^{-\gamma}(\omega(t_k-s)^{\rho})(f(s)-P_j(s))\mathrm{d}s\\
&=\sum_{j=1}^{r-1}\frac{f^{(j+1)}(\xi)}{(j+1)!}\int_{t_{j-1}}^{t_j}(s-t_j)(s-t_{j-1})\dots(s-t_0)(t_k-s)^{-\alpha-1}E_{\rho,-\alpha}^{-\gamma}(\omega(t_k-s)^{\rho})\mathrm{d}s\\
&\leq\sum_{j=1}^{r-1}-\frac{f^{(j+1)}(\xi)}{4(j+1)!}\tau^{j+1}j!\int_{t_{j-1}}^{t_j}(t_k-s)^{-\alpha-1}E_{\rho,-\alpha}^{-\gamma}(\omega(t_k-s)^{\rho})\mathrm{d}s\\
&\leq\sum_{j=1}^{r-1}-\frac{f^{(j+1)}(\xi)}{4(j+1)}\tau^{j+1-\alpha}\Big[(k-j)^{-\alpha}E_{\rho,1-\alpha}^{-\gamma}(\omega(t_k-t_j)^{\rho})\\
&\quad-(k-j+1)^{-\alpha}E_{\rho,1-\alpha}^{-\gamma}(\omega(t_k-t_{j-1})^{\rho})\Big].
\end{aligned}\tag{10}$$

Now we will consider the second integral:

$$\begin{aligned}
&\sum_{j=r}^{k-1}\int_{t_{j-1}}^{t_j}(t_k-s)^{-\alpha-1}E_{\rho,-\alpha}^{-\gamma}(\omega(t_k-s)^{\rho})(f(s)-P_r(s))'\mathrm{d}s\\
&=\sum_{j=r}^{k-1}\int_{t_{j-1}}^{t_j}\frac{f^{(r+1)}(\xi)}{(r+1)!}(s-t_j)(s-t_{j-1})\dots(s-t_{j-r})(t_k-s)^{-\alpha-1}E_{\rho,-\alpha}^{-\gamma}(\omega(t_k-s)^{\rho})\mathrm{d}s
\end{aligned}$$

$$\leq \sum_{j=r}^{k-1} -\frac{f^{(r+1)}(\xi)}{(r+1)!}\frac{\tau^{r+1}}{4} r! \int_{t_{j-1}}^{t_j} (t_k - s)^{-\alpha-1} E^{-\gamma}_{\rho,-\alpha}(\omega(t_k - s)^{\rho}) \mathrm{d}s$$

$$\leq \sum_{j=r}^{k-1} -\frac{f^{(r+1)}(\xi)}{4(r+1)} \tau^{r+1-\alpha} \Big[(k-j)^{-\alpha} E^{-\gamma}_{\rho,1-\alpha}(\omega(t_k - t_j)^{\rho})$$

$$- (k-j+1)^{-\alpha} E^{-\gamma}_{\rho,1-\alpha}(\omega(t_k - t_{j-1})^{\rho}) \Big]. \tag{11}$$

Next we consider the third integral:

$$\int_{t_{k-1}}^{t_k} (t_k - s)^{-\alpha-1} E^{-\gamma}_{\rho,-\alpha}(\omega(t_k - s)^{\rho})(f(s) - P_r(s)) \mathrm{d}s$$

$$= \frac{f^{(r+1)}(\xi)}{(r+1)!} \int_{t_{k-1}}^{t_k} (s - t_k)(s - t_{k-1}) \dots (s - t_{k-r})(t_k - s)^{-\alpha-1} E^{-\gamma}_{\rho,-\alpha}(\omega(t_k - s)^{\rho})$$

$$\leq -\frac{f^{(r+1)}(\xi)}{(r+1)!} r! \frac{\tau^{r+1}}{4} \int_{t_{k-1}}^{t_k} (t_k - s)^{-\alpha-1} E^{-\gamma}_{\rho,-\alpha}(\omega(t_k - s)^{\rho}) \mathrm{d}s$$

$$\leq -\frac{f^{(r+1)}(\xi)}{r+1} \frac{\tau^{r+1-\alpha}}{4} E^{-\gamma}_{\rho,1-\alpha}(\tau^{\rho}). \tag{12}$$

Now combining (10)–(12), we get

$$\begin{aligned} \left|E_r^k\right| \leq & \left| \sum_{j=1}^{r-1} \frac{f^{(j+1)}(\xi)}{4(j+1)} \tau^{j+1-\alpha} \Big[(k-j)^{-\alpha} E^{-\gamma}_{\rho,1-\alpha}(\omega(t_k - t_j)^{\rho}) \right. \\ & \left. - (k-j+1)^{-\alpha} E^{-\gamma}_{\rho,1-\alpha}(\omega(t_k - t_{j-1})^{\rho}) \Big] \right| \\ & + \left| \sum_{j=r}^{k-1} \frac{f^{(r+1)}(\xi)}{4(r+1)} \tau^{r+1-\alpha} \Big[(k-j)^{-\alpha} E^{-\gamma}_{\rho,1-\alpha}(\omega(t_k - t_j)^{\rho}) \right. \\ & \left. - (k-j+1)^{-\alpha} E^{-\gamma}_{\rho,1-\alpha}(\omega(t_k - t_{j+1})^{\rho}) \Big] \right| + \left| \frac{f^{(r+1)}(\xi)}{r+1} \frac{\tau^{r+1-\alpha}}{4} E^{-\gamma}_{\rho,1-\alpha}(\tau^{\rho}) \right| \\ \leq & C_4 \max_{t_0 \leq t \leq t_k} \left| f^{(r+1)}(t) \right| \tau^{r+1-\alpha}, \end{aligned}$$

where C_4 is a positive constant.

This completes the proof. □

2.2 Numerical experiments

Here, we discuss two test examples in order to validate the numerical algorithm established in this paper. Numerical results for $r = 4$ and $r = 5$ are given in this paper. To calculate the maximum absolute error ϵ, we use the formula

$$\epsilon_i^k = \max_{1 \leq k \leq M} \max_{1 \leq i \leq N-1} \left| u_i^k - U_i^k \right|, \tag{13}$$

where U_i^k and u_i^k are the analytical and numerical solutions, respectively. To calculate the order of convergence

$\mathbb{O}$, we use the formula

$$\mathbb{O}(j) = \begin{cases} \dfrac{\log\left(\epsilon(j)/\epsilon(j+1)\right)}{\log(\tau(j)/\tau(j+1))}, & \text{in time direction,} \\ \dfrac{\log\left(\epsilon(j)/\epsilon(j+1)\right)}{\log(h(j)/h(j+1))}, & \text{in space direction.} \end{cases} \tag{14}$$

When the analytical solution is unknown, we calculate the convergence order using the (see [40]) formula

$$CO(j) = \log_2\left(\frac{\Delta e_j}{\Delta e_{\frac{j}{2}}}\right), \tag{15}$$

where $\Delta e_j = e_j - e_{\frac{j}{2}}$, and e_j is the error calculated at the jth step size.

Example 1. For the function $f(t) = t^6, t \in [0, T]$, calculate the αth-order Caputo–Prabhakar derivative for $0 < \alpha < 1$. The exact solution is ${}_0^{CP}D^{\gamma}_{\rho,\alpha,\omega} t^6 = 720 t^{6-\alpha} E^{-\gamma}_{\rho,7-\alpha}(\omega t^{\rho})$. Since $f \in L^1[0,1]$, its Caputo–Prabhakar derivative can be calculated. For $r = 4, 5$, we have calculated the maximum absolute error and the convergence rate at $T = 1$, for different $\alpha = 0.2, 0.4, 0.6, 0.8$, and step sizes $\tau = 1/10, 1/20, 1/40, 1/80, 1/160$ and listed the obtained results in Table 1. It is evident from Table 1 that the computational convergence rate is $(r + 1 - \alpha)$, and this validates our analytical results.

Example 2. Calculate the αth order Caputo–Prabhakar derivative of $f(t) = t^{(7-\alpha)}$, $t \in [0, T]$ at $T = 1$, for $0 < \alpha < 1$. The analytical expression of the Caputo–Prabhakar derivative of order α for the function f is unknown. So the convergence order of f is calculated with the help of the formula (15) at the various step sizes $\tau = 1/10, 1/20, 1/40, 1/80, 1/160$, for $r = 4, 5$. Results obtained for various values of $\alpha = 0.2, 0.4, 0.6, 0.8$ are given in Tables 2 and 3. From these tables, it is evident that convergence is of order $(r + 1 - \alpha)$.

Table 1: Maximum absolute error and convergence rate for different α with $r = 4, 5$ for Ex. 1.

α	$\frac{1}{\tau}$	$r = 4$		$r = 5$	
		Error	**Rate**	**Error**	**Rate**
	10	2.17269E-04		5.61268E-05	
	20	9.20339E-06	4.561170047	1.00321E-06	5.806000930
$\alpha = 0.2$	40	3.65401E-07	4.654611755	1.79348E-08	5.805708873
	80	1.40569E-08	4.700136700	3.20696E-10	5.805415154
	160	5.07831E-10	4.790780758	5.73104E-12	5.806265187
	10	8.27842E-04		2.21479E-04	
	20	3.87247E-05	4.418030780	4.53034E-06	5.611402754
$\alpha = 0.4$	40	1.70510E-06	4.505322512	9.27205E-08	5.610588178
	80	7.29072E-08	4.547654752	1.89866E-09	5.609834164
	160	3.08555E-09	4.562458941	3.85654E-11	5.621532192
	10	2.33224E-03		6.38322E-04	
	20	1.22530E-04	4.250506895	1.49810E-05	5.413076890
$\alpha = 0.6$	40	6.08656E-06	4.331364719	3.51831E-07	5.412107834
	80	2.94567E-07	4.368959695	8.26791E-09	5.411216612
	160	1.41958E-08	4.375065330	1.92069E-10	5.427826916
	10	5.85829E-03		1.62573E-03	
	20	3.49316E-04	4.067876660	4.38035E-05	5.213899935
$\alpha = 0.8$	40	1.97627E-05	4.143679974	1.18109E-06	5.212856507
	80	1.09192E-06	4.177848534	3.18672E-08	5.211898995
	160	5.96854E-08	4.193339720	8.60343E-10	5.211019274

Table 2: Convergence order for $r = 4$ and $\alpha = 0.2, 0.4, 0.6, 0.8$ for Ex. 2.

α	t	CO		
		$\log_2\left(\frac{\Delta e_\tau}{\Delta e_{\tau/2}}\right)$	$\log_2\left(\frac{\Delta e_{\tau/2}}{\Delta e_{\tau/4}}\right)$	$\log_2\left(\frac{\Delta e_{\tau/4}}{\Delta e_{\tau/8}}\right)$
$\alpha = 0.2$	0.2	3.297043141	3.887934476	4.361720732
	0.4	3.888133923	4.361918662	4.556786856
	0.6	4.218662364	4.494017638	4.618913879
	0.8	4.362117231	4.556988293	4.650393851
	1.0	4.442533787	4.594261524	4.670392859
$\alpha = 0.4$	0.2	3.264374227	3.822539836	4.254058831
	0.4	3.823136148	4.254638139	4.426802609
	0.6	4.126252583	4.372041805	4.480815299
	0.8	4.255263575	4.427413193	4.507724918
	1.0	4.326919661	4.459925372	4.524054787
$\alpha = 0.6$	0.2	3.235120944	3.742039586	4.124920093
	0.4	3.742828549	4.125688384	4.273196362
	0.6	4.013709373	4.226914468	4.318464967
	0.8	4.126523236	4.274001342	4.340676012
	1.0	4.188499651	4.301351990	4.354152176
$\alpha = 0.8$	0.2	3.213208179	3.650175565	3.980696208
	0.4	3.651097925	3.981586111	4.104707046
	0.6	3.886572972	4.066579453	4.141783413
	0.8	3.982555474	4.105626746	4.159681977
	1.0	4.034739895	4.128097929	4.170262620

Table 3: Convergence order for $r = 5$ and $\alpha = 0.2, 0.4, 0.6, 0.8$ for Ex. 2.

α	t	CO		
		$\log_2\left(\frac{\Delta e_\tau}{\Delta e_{\tau/2}}\right)$	$\log_2\left(\frac{\Delta e_{\tau/2}}{\Delta e_{\tau/4}}\right)$	$\log_2\left(\frac{\Delta e_{\tau/4}}{\Delta e_{\tau/8}}\right)$
0.2	0.2	3.178154561	6.144325501	5.491391524
	0.4	6.144517302	5.491580755	5.628329508
	0.6	5.382954534	5.585449054	5.666258000
	0.8	5.491771047	5.628486888	5.635934183
	1.0	5.549527543	5.652521217	5.657650319
0.4	0.2	3.151015664	6.224331038	5.401914777
	0.4	6.224921790	5.402488712	5.503817556
	0.6	5.320493092	5.472613052	5.532773242
	0.8	5.403108203	5.504393645	5.492497663
	1.0	5.446397986	5.522341012	5.509000913
0.6	0.2	3.125306042	6.307152597	5.287134506
	0.4	6.307958643	5.287910878	5.353002477
	0.6	5.233918644	5.333512549	5.372085958
	0.8	5.288754480	5.353832890	5.409466499
	1.0	5.317027438	5.365603651	5.415207771
0.8	0.2	3.104259189	6.403641612	5.154936411
	0.4	6.404603609	5.155840054	5.186548904
	0.6	5.129777704	5.177878033	5.192206296
	0.8	5.156824473	5.187506576	5.165950915
	1.0	5.170546613	5.192738576	5.169693848

3 Application 1: fractional advection–diffusion equation

In this section, we use the high-order numerical scheme discussed in Section 2 for solving the time fractional advection–diffusion equation

$$\begin{cases} {}_0^{CP}D^{\gamma}_{\rho,\alpha,\omega}u(x,t) = K\dfrac{\partial^2 u(x,t)}{\partial x^2} - V\dfrac{\partial u(x,t)}{\partial x} + f(x,t), \qquad 0 < x < L,\ 0 < t < T, \\ u(x,0) = u_0(x), \\ u(0,t) = \eta_1(t), \\ u(L,t) = \eta_2(t), \end{cases} \tag{16}$$

where $V > 0$, $K > 0$ and $f(x,t)$ are the average fluid velocity, diffusion coefficient and the source term, respectively. Here, $f(x,t)$, $u_0(x)$, $\eta_1(t)$ and $\eta_2(t)$ are the sufficiently smooth known functions and $u \in C^{(2,r)}_{(x,t)}([0,L]\times[0,T])$. The spatial domain $[0,L]$ is discretized into $N \in \mathbb{N}$ subdomains by choosing a partition $0 = x_0 < x_1 < \ldots < x_N = L$ of uniform length $h = \frac{L}{N}$ such that $x_i = ih$, for $i = 0, 1, \ldots, N$. Let the analytical and approximate solution of $u(x,t)$ at the node (x_i, t_k) be U_i^k and u_i^k respectively. The first and the second-order derivatives in space are approximated using the central difference scheme:

$$\frac{\partial u(x_i,t_k)}{\partial x} = \frac{U_{i+1}^k - U_{i-1}^k}{2h} + O(h^2), \tag{17}$$

$$\frac{\partial^2 u(x_i,t_k)}{\partial x^2} = \frac{U_{i+1}^k - 2U_i^k + U_{i-1}^k}{h^2} + O(h^2). \tag{18}$$

By using (6), the time fractional Caputo–Prabhakar derivative term in (16) is approximated as

$${}_0^{CP}D^{\gamma}_{\rho,\alpha,\omega}u(x_i,t_k) = \tau^{-\alpha}\sum_{j=0}^{k} p_{k-j}^r U_i^j + O(\tau^{r+1-\alpha}). \tag{19}$$

By omitting the truncation error terms in (17)–(19), and replacing the analytical solution with numerical one, we get the finite difference scheme for the numerical solution of (16) as

$$\tau^{-\alpha}\sum_{j=0}^{k} p_{k-j}^r u_i^j = K\frac{u_{i+1}^k - 2u_i^k + u_{i-1}^k}{h^2} - V\frac{u_{i+1}^k - u_{i-1}^k}{2h} + f_i^k,$$

which again can be written as

$$\left(K - \frac{Vh}{2}\right)u_{i+1}^k + \left(-2K - h^2\tau^{-\alpha}p_0^r\right)u_i^k + \left(K + \frac{Vh}{2}\right)u_{i-1}^k + h^2 f_i^k = h^2\tau^{-\alpha}\sum_{j=0}^{k-1} p_{k-j}^r u_i^j, \tag{20}$$

where $1 \le i \le N-1$ and $1 \le k \le M$. Also from (16),

$$u_i^0 = u_0(x_i), \quad 0 \le i \le N, \tag{21}$$

$$\begin{cases} u_0^k = \eta_1(t_k), \\ u_N^k = \eta_2(t_k), \quad 1 \le k \le M. \end{cases} \tag{22}$$

Let $h^2\tau^{-\alpha} = \mu$. Then,

$$\begin{cases} \left(-K - \frac{Vh}{2}\right) & u_{i-1}^1 + (2K + \mu p_0^r)u_i^1 + \left(-K + \frac{Vh}{2}\right)u_{i+1}^1 \\ & = -\mu p_1^r u_i^0 + h^2 f_i^1, \qquad k = 1, \\ \vdots & \\ \left(-K - \frac{Vh}{2}\right) & u_{i-1}^{r-1} + (2K + \mu p_0^r)u_i^{r-1} + \left(-K + \frac{Vh}{2}\right)u_{i+1}^{r-1} \\ & = -\mu \sum_{j=0}^{r-2} p_{k-j}^r u_i^j + h^2 f_i^{r-1}, \qquad k = r-1, \\ \left(-K - \frac{Vh}{2}\right) & u_{i-1}^k + (2K + \mu p_0^r)u_i^k + \left(-K + \frac{Vh}{2}\right)u_{i+1}^k \\ & = -\mu \sum_{j=0}^{k-1} p_{k-j}^r u_i^j + h^2 f_i^k, \qquad k \geq r. \end{cases} \tag{23}$$

Equation (23) can be written in matrix form as

$$\begin{cases} AU^1 = -\mu P_1^r U^0 + h^2 F^1 + B^1, & k = 1, \\ \vdots & \\ AU^{r-1} = -\mu P_{r-1}^r U^{r-2} + h^2 F^{r-1} + B^{r-1}, & k = r-1, \\ AU^k = -\mu P_k^r U^{k-1} + h^2 F^k + B^k, & k \geq r. \end{cases} \tag{24}$$

The matrix and the vectors in (24) are given as

$$\begin{aligned} A &= \operatorname{tri}\left[\left(-K - \frac{Vh}{2}\right), \quad (2K + \mu p_0^r), \quad \left(-K + \frac{Vh}{2}\right)\right], \\ U^k &= \left[u_1^k, \ldots, u_{n-1}^k\right], \\ P_k^r &= \left[p_k^r, \ldots, p_1^r\right]^T, \\ F^k &= \left[f_1^k, f_2^k, \ldots, f_{N-1}^k\right], \\ B^k &= \left[\left(K + \frac{Vh}{2}\right)u_0^k, \ldots, \left(K - \frac{Vh}{2}\right)u_N^k\right], \qquad 1 \leq k \leq M. \end{aligned}$$

3.1 Stability analysis

Without loss of generality, we study stability analysis of the finite difference scheme (24) for $r = 4$, using von Neumann stability analysis. For other values of $4 \geq r \in \mathbb{N}$, this study follows similarly. Let $\hat{u}_i^k$ be the approximate solution of (24) and define

$$\delta_i^k = u_i^k - \hat{u}_i^k, \ i = 1, 2, \ldots, N-1, \quad k = 1, 2, \ldots, M,$$

with the corresponding vector

$$\delta^k = \left[\delta_1^k, \delta_2^k, \ldots, \delta_{N-1}^k\right]^T.$$

The error equations are obtained as

$$\begin{cases} \left(-K-\frac{Vh}{2}\right)\delta_{i-1}^{1}+\left(2K+\mu p_0^r\right)\delta_i^1+\left(-K+\frac{Vh}{2}\right)\delta_{i+1}^{1}=-\mu p_1^r\delta_i^0,\ k=1,\\ \vdots\\ \left(-K-\frac{Vh}{2}\right)\delta_{i-1}^{r-1}+\left(2K+\mu p_0^r\right)\delta_i^{r-1}+\left(-K+\frac{Vh}{2}\right)\delta_{i+1}^{r-1}=-\mu\sum_{j=0}^{r-2}p_{k-j}^r\delta_i^j,\ k=r-1,\\ \left(-K-\frac{Vh}{2}\right)\delta_{i-1}^{k}+\left(2K+\mu p_0^r\right)\delta_i^k+\left(-K+\frac{Vh}{2}\right)\delta_{i+1}^{k}=-\mu\sum_{j=0}^{k-1}p_{k-j}^r\delta_i^j,\ k\geq r. \end{cases} \tag{25}$$

To check the stability using von Neumann method, let us assume $\delta_i^k=d_k e^{I\sigma ih}$, where σ is the wave number and $I=\sqrt{-1}$. From (25), we have

$$\begin{cases} d_1=\dfrac{-\mu p_1^r d_0}{4K\,\sin^2\left(\frac{\sigma h}{2}\right)+IVh\,\sin(\sigma h)+\mu p_0^r},\quad k=1,\\ \vdots\\ d_{r-1}=\dfrac{-\mu\sum_{j=0}^{r-2}p_{k-j}^r d_j}{4K\,\sin^2\left(\frac{\sigma h}{2}\right)+IVh\,\sin(\sigma h)+\mu p_0^r},\ k=r-1,\\ d_k=\dfrac{-\mu\sum_{j=0}^{k-1}p_{k-j}^r d_j}{4K\,\sin^2\left(\frac{\sigma h}{2}\right)+IVh\,\sin(\sigma h)+\mu p_0^r},\quad k\geq r. \end{cases} \tag{26}$$

Now we use the idea of mathematical induction to prove that $|d_k|\leq|d_0|$ for all k. Observe that

$$\left|4K\,\sin^2\left(\frac{\sigma h}{2}\right)+IVh\,\sin(\sigma h)+\mu p_0^r\right|=\sqrt{\left(4K\,\sin^2\left(\frac{\sigma h}{2}\right)+\mu p_0^r\right)^2+V^2h^2\,\sin^2(\sigma h)},$$
$$\geq\sqrt{\mu^2\left(p_0^r\right)^2}=\mu p_0^r.$$

Now, for $k=1$,

$$|d_1|=\left|\frac{-\mu p_1^r d_0}{4K\,\sin^2\left(\frac{\sigma h}{2}\right)+IVh\,\sin(\sigma h)+\mu p_0^r}\right|\leq\left|\frac{-\mu p_1^r d_0}{\mu p_0^r}\right|$$

by property 1 of Lemma 1, $|d_1|\leq|d_0|$. Let us suppose that $|d_j|\leq|d_0|$ for $2\leq j\leq k-1$. Hence, from (26), we have

$$|d_k|=\left|\frac{-\mu}{4K\,\sin^2\left(\frac{\sigma h}{2}\right)+IVh\,\sin(\sigma h)+\mu p_0^r}\sum_{j=0}^{k-1}p_{k-j}^r d_j\right|$$
$$\leq\left|\frac{-\mu d_0}{4K\,\sin^2\left(\frac{\sigma h}{2}\right)+IVh\,\sin(\sigma h)+\mu p_0^r}\sum_{j=1}^{k}p_j^r\right|$$

by property 2 of Lemma 1,

$$|d_k|\leq\frac{\mu|d_0|}{4K\,\sin^2\left(\frac{\sigma h}{2}\right)+IVh\,\sin(\sigma h)+\mu p_0^r}\sum_{j=1}^{k}\left|p_j^r\right|,$$

$$\leq \frac{\mu p_0^r |d_0|}{4K \sin^2\left(\frac{\sigma h}{2}\right) + IVh \sin(\sigma h) + \mu p_0^r} \leq \frac{\mu p_0^r |d_0|}{\mu p_0^r} = |d_0|,$$

which establishes that the finite difference scheme (24) is stable.

3.2 Uniqueness and existence

Here we discuss the uniqueness and existence of the solution of the finite difference scheme (24).

Lemma 2. *The coefficient matrix A in* (24) *is invertible.*

Proof. Without loss of generality, we will prove this for $r = 4$, and for other values of $4 \leq r \in \mathbb{N}$, the proof follows in a similar way. A tridiagonal matrix of the form $\text{tri}\begin{bmatrix} z & x & y \end{bmatrix}$ has eigenvalues [41, pg. 154] given as

$$\lambda_j = x + 2y\left(\frac{z}{y}\right)^{1/2} \cos\left(\frac{j\pi}{N}\right), \quad j = 1, 2, \ldots, N-1. \tag{27}$$

The coefficient matrix A of the finite difference scheme is

$$A = \text{tri}\left[-K - \frac{Vh}{2}, \quad 2K + \mu p_0^r, \quad -K + \frac{Vh}{2}\right].$$

By (27), the eigenvalues of A are

$$\lambda_j = 2K + \mu p_0^r + 2\sqrt{K^2 - \frac{V^2h^2}{4}} \cos\left(\frac{j\pi}{N}\right), \quad j = 1, 2, \ldots, N-1.$$

Case (1.) If $K^2 - \frac{V^2h^2}{4} \leq 0$, then the eigenvalues of A are of the form $\lambda_j = \Upsilon_1 + i\Upsilon_2$, where $\Upsilon_1 = 2K + \mu p_0^r$ and $i^2 = -1$. $K > 0$ and $\mu = h^2\tau^{-\alpha} > 0$ and $p_0^r = W_{0,0}^r > 0$ if $\omega > 0$, so, $\Upsilon_1 > 0$ if $\omega > 0$. So, $\lambda_j \neq 0$ if $\omega > 0$.

Case (2.) If $K^2 - \frac{V^2h^2}{4} > 0$, then

$$\lambda_j = 2K + \mu p_0^r + 2\sqrt{K^2 - \frac{V^2h^2}{4}} \cos\left(\frac{j\pi}{N}\right) \geq 2K + \mu p_0^r + 2K > 0,$$

if $\omega > 0$. So, $\lambda_j \neq 0$ if $\omega > 0$.

In both cases, the eigenvalues of A are nonzero, so A is invertible. □

Theorem 2. *There exists a unique solution of the given schemes for all values of r.*

Proof. To solve the finite difference scheme (24) at t_k, we need to solve the system of linear equations with coefficient matrix A. Lemma 2 shows that the matrix A is invertible. So there always exists a unique solution of the corresponding system of linear equations and, hence the solution of (24) always exists and is unique. □

3.3 Convergence analysis

We study convergence analysis of the numerical method for $r = 4$, and for other values of r, the proof follows similarly. From (24), the numerical solution of the problem is obtained as

$$AU^k = -\mu P_k^r U^{k-1} + h^2 F^k + B^k + O(h^2, \tau^{r+1-\alpha}), \ k \geq r. \tag{28}$$

Let u^k be the exact solution so that

$$Au^k = -\mu P_k^r u^{k-1} + h^2 F^k + B^k, \ k \geq r. \tag{29}$$

The error equation is

$$A(U^k - u^k) = -\mu P_k^r (U^{k-1} - u^{k-1}) + O(h^2, \tau^{r+1-\alpha})$$

$$A\epsilon^k = -\mu P_k^r \epsilon^{k-1} + O(h^2, \tau^{r+1-\alpha})$$

$$\epsilon^k = -\mu A^{-1} P_k^r \epsilon^{k-1} + O(h^2, \tau^{r+1-\alpha}) A^{-1}.$$

Let $O(h^2, \tau^{r+1-\alpha})A^{-1} = b$ so that

$$\epsilon^k = -\mu A^{-1} P_k^r \epsilon^{k-1} + b. \tag{30}$$

Since $\epsilon^0 = 0$, we get

$$\begin{aligned}
&\epsilon^1 = b \\
&\epsilon^2 = (-\mu A^{-1}) P_2^r \epsilon^1 + b = ((-\mu A^{-1}) P_2^r + I) b \\
&\epsilon^3 = (-\mu A^{-1}) P_3^r \epsilon^2 + b = ((-\mu A^{-1})^2 P_2^r P_3^r + (-\mu A^{-1}) P_3^r + I) b \\
&\vdots \\
&\epsilon^k = ((-\mu A^{-1})^{k-1} P_k^r P_{k-1}^r \dots P_2^r + (-\mu A^{-1})^{k-2} P_k^r \dots P_3^r + \dots + (-\mu A^{-1}) P_k^r + I) b.
\end{aligned}$$

Hence,

$$\begin{aligned}
\| \epsilon^k \| \le \Big(&\left| -\mu^{k-1} \right| \| \left(A^{-1} \right)^{k-1} \| \| P_k^r \| \| P_{k-1}^r \| \dots \| P_2^r \| \\
&+ \left| -\mu^{k-2} \right| \| \left(A^{-1} \right)^{k-2} \| \| P_k^r \| \| P_{k-1}^r \| \dots \| P_3^r \| + \dots \\
&+ |-\mu| \| A^{-1} \| \| P_k^r \| + 1 \Big) \| A^{-1} \| O(h^2, \tau^{r+1-\alpha}).
\end{aligned} \tag{31}$$

Now, the matrix A is tridiagonal matrix given by

$$A = \text{tri}\left[\left(-K - \frac{Vh}{2} \right), \quad (2K + \mu p_0^r), \quad \left(-K + \frac{Vh}{2} \right) \right],$$

which is strictly diagonally dominant under the assumption that $(K - \frac{Vh}{2}) > 0$, and hence

$$\| A^{-1} \| \le \frac{1}{\min_{i \in N} \{ |a_{ii}| - R_i(A) \}},$$

where $R_i(A)$ is the absolute sum of elements of the ith-row except the diagonal entry of matrix A [42]. For the matrix A, $\min_{i \in N} \{ |a_{ii}| - R_i(A) \} = \mu p_0^r = C'$, so

$$\| A^{-1} \| \le \frac{1}{C'} = C. \tag{32}$$

Now, $P_k^r = \left[p_k^r \;\; p_{k-1}^r \;\; \dots \;\; p_1^r \;\; p_o^r \right]$, so $\|P_k^r\| = \max_i \{ p_i^r \}$. Since each p_i^r is an infinite series or sum of infinite series and every such infinite series is convergent, we get

$$\| P_k^r \| = C_k. \tag{33}$$

From (31)–(33), we have

$$\| \epsilon^k \| \le C \; O(h^2, \tau^{r+1-\alpha}), \;\; k \ge r.$$

So the given scheme converges conditionally.

3.4 Numerical experiments

Here, we present a numerical example to validate the numerical scheme (24) for values of $r = 4$ and $r = 5$. For numerical computations, we have used (13) and (14).

Example 3. Let us consider (16) in the domain $[0,1] \times [0,1]$, with $u(x,0) = 0$ and $u(0,t) = u(1,t) = 0$. $f(x,t) = 720\cos(\pi x + \frac{\pi}{2})t^{6-\alpha}E^{-\gamma}_{\rho,7-\alpha}(\omega t^{\rho}) + \pi^2 t^6\cos(\pi x + \frac{\pi}{2}) - \pi t^6\sin(\pi x + \frac{\pi}{2})$ is the source term and $u(x,t) = t^6\cos(\pi x + \frac{\pi}{2})$ is the exact solution. The convergence order is calculated for different values of α and h in the spatial direction with fixed temporal step size $\tau = 1/500$. The obtained results are presented in Table 4, which shows that the convergence order in the spatial direction is $O(h^2)$. Again, we have calculated the temporal convergence order for different values of τ and for fixed $h = 1/3000$. The results are shown in Table 5, which validates our theoretical finding of the temporal convergence rate $O(\tau^{r+1-\alpha})$. Figure 1 gives a comparison between numerical solutions for $r = 4, 5$ and the analytical solution, for the step sizes $h = \tau = 1/500$ and $\alpha = 0.5$.

Table 4: Maximum absolute error and convergence rate for different h and α and fixed $1/\tau = 500$ for Ex. 3.

α	$\frac{1}{h}$	$r = 4$		$r = 5$	
		Error	**Rate**	**Error**	**Rate**
$\alpha = 0.2$	10	7.17970E-03		7.17971E-03	
	20	1.80819E-03	1.989380393	1.80819E-03	1.989375017
	40	4.51788E-04	2.000824231	4.51798E-04	2.000802433
	80	1.12935E-04	2.000156777	1.12944E-04	2.000068458
	160	2.82379E-05	1.999782727	2.82471E-05	1.999432898
$\alpha = 0.4$	10	6.73107E-03		6.73108E-03	
	20	1.69931E-03	1.985890047	1.69932E-03	1.985881175
	40	4.24623E-04	2.000692077	4.24637E-04	2.000656089
	80	1.06143E-04	2.000174473	1.06157E-04	2.000030529
	160	2.65348E-05	2.000049144	2.65489E-05	1.999473483
$\alpha = 0.6$	10	6.18959E-03		6.18960E-03	
	20	1.56359E-03	1.984976000	1.56361E-03	1.984968852
	40	3.90758E-04	2.000522538	3.90768E-04	2.000494328
	80	9.76807E-05	2.000129606	9.76909E-05	2.000016772
	160	2.44196E-05	2.000027891	2.44299E-05	1.999576680
$\alpha = 0.8$	10	5.56161E-03		5.56160E-03	
	20	1.40059E-03	1.989462817	1.40059E-03	1.989471007
	40	3.50073E-04	2.000312302	3.50063E-04	2.000344602
	80	8.75540E-05	1.999410558	8.75437E-05	1.999537879
	160	2.18883E-05	2.000009225	2.18780E-05	2.000520468

Table 5: Maximum absolute error and convergence rate for $\alpha = 0.2$ and $1/h = 3000$ for Ex. 3.

$\frac{1}{\tau}$	$r = 4$		$r = 5$	
	Error	**Rate**	**Error**	**Rate**
10	1.91777E-05		3.31267E-03	
12	8.01857E-06	4.782686729	1.10886E-03	6.002685927
14	3.83332E-06	4.787715519	4.39555E-04	6.002746887
16	2.03015E-06	4.760094023	1.97197E-04	6.002799499
18	1.15433E-06	4.793431493	9.72386E-05	6.002845811

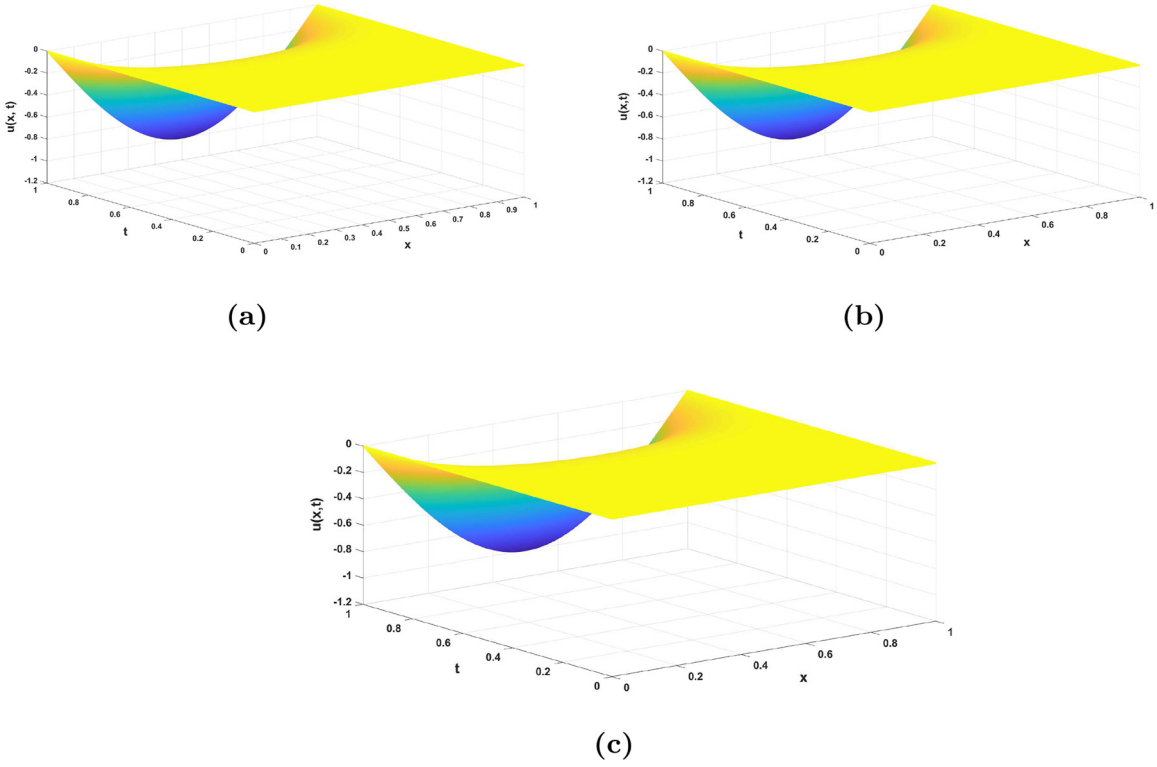

Figure 1: Numerical and analytical solutions when $\alpha = 0.5$ for Ex. 3. (a) Numerical solution when $r = 4$. (b) Numerical solution when $r = 5$. (c) Analytical solution.

4 Application 2: fractional reaction–diffusion equation

In the present section, we apply the discussed high-order numerical method to solve the nonlinear time fractional reaction–diffusion equation

$$\begin{cases} {}_0^{CP}D^{\gamma}_{\rho,\alpha,\omega}u(x,t) = K\dfrac{\partial^2 u(x,t)}{\partial x^2} + f(u) + g(x,t), \qquad 0 < x < L,\ 0 < t < T, \\ u(x,0) = \varphi_0(x), \\ u(0,t) = 0, \\ u(L,t) = 0, \end{cases} \tag{34}$$

where $K > 0$ is the diffusion coefficient and $f(u)$ is the reaction term satisfying the Lipschitz condition

$$|f(u_1) - f(u_2)| \le L|u_1 - u_2| \quad \forall u_1, u_2 \in [0, L] \times [0, T],$$

with $L > 0$ as Lipschitz constant. $\varphi_0(x)$ and $g(x,t)$ are the sufficiently smooth known functions. Using (17)–(19) at node point (x_i, t_k), we get the finite difference equation

$$\tau^{-\alpha}\sum_{j=0}^{k} p^r_{k-j}U^j_i = \frac{K}{h^2}\left(U^k_{i+1} - 2U^k_i + U^k_{i-1}\right) + f(U^k_i),$$

$$KU^k_{i+1} + \left(-2K - h^2\tau^{-\alpha}p^r_0\right)U^k_i + KU^k_{i-1} + h^2 f(U^k_i)$$

$$= h^2\tau^{-\alpha}\sum_{j=0}^{k-1} p_{k-j}^{r} U_i^j - h^2 g(x_i, t_k) + R_i^k, \tag{35}$$

where $|R_i^k| \le C(\tau^{r+1-\alpha}, h^2)$, $1 \le i \le N-1$, $r \le k \le N$ and $C > 0$ is a positive constant. Omitting the small terms R_i^n and replacing the analytical solution with the numerical one, we get the scheme

$$Ku_{i+1}^k + \left(-2K - h^2\tau^{-\alpha} p_0^r\right)u_i^k + Ku_{i-1}^k + h^2 f(u_i^k) = h^2\tau^{-\alpha}\sum_{j=0}^{k-1} p_{k-j}^{r} u_i^j - h^2 g(x_i, t_k), \tag{36}$$

which again can be written in the matrix form as

$$A^k U^k + h^2 I_{N-1} f(U^k) = h^2\tau^{-\alpha}\sum_{j=0}^{k-1} p_{k-j}^{r} U^j - h^2 G^k, \tag{37}$$

where

$$A^k = \operatorname{diag}\begin{bmatrix} K & -2K - h^2\tau^{-\alpha} p_0^r & K \end{bmatrix},\ U^k = \begin{bmatrix} u_1^k & u_2^k & \dots & u_{N-1}^k \end{bmatrix}^T,$$
$$f(U^k) = \begin{bmatrix} f(u_1^k) & f(u_2^k) & \dots & f(u_{N-1}^k) \end{bmatrix}^T,\ G^k = \begin{bmatrix} g_1^k & g_2^k & \dots & g_{N-1}^k \end{bmatrix}^T.$$

Now, we use the Newton–Raphson method for solving (37). To apply the Newton–Raphson method, the iterative form of (37) is obtained as

$$A^k U^{[k,s+1]} + h^2 I_{N-1} f(U^{[k,s+1]}) = h^2\tau^{-\alpha}\sum_{j=0}^{k-1} p_{k-j}^{r} U^j - h^2 G^k. \tag{38}$$

Using Newton's iterative method, $f(U^{[k,s+1]})$ can be written as

$$f(U^{[k,s+1]}) = f(U^{[k,s]}) + (U^{[k,s+1]} - U^{[k,s]}) f'(U^{[k,s]}). \tag{39}$$

From (38) and (39), we get

$$\left[A^k + h^2 I_{N-1} f'(U^{[k,s]})\right] U^{[k,s+1]} = h^2 I_{N-1}\left[U^{[k,s]} f'(U^{[k,s]}) - f(U^{[k,s]})\right] + h^2\tau^{-\alpha}\sum_{j=0}^{k-1} p_{k-j}^{r} U^j - h^2 G^k, \tag{40}$$

where $U^{[k,s]}$ is the value at kth-time level of sth-iteration.

4.1 Stability analysis

Theorem 3. *The proposed numerical scheme* (36) *is stable for* $\alpha \in (0, 1)$.

Proof. Here, we prove that the given numerical scheme is stable using von Neumann stability analysis. Let $\hat{u}$ be the perturbed solution, which is obtained by adding the perturbation term ϑ_i^k defined as $\vartheta_i^k = u_i^k - \hat{u}_i^k$. From (36), the perturbation term satisfies the equation

$$K\vartheta_{i+1}^k + \left(-2K - h^2\tau^{-\alpha} p_0^r\right)\vartheta_i^k + K\vartheta_{i-1}^k = h^2\tau^{-\alpha}\sum_{j=0}^{k-1} p_{k-j}^{r}\tau_i^j - h^2(f(u_i^k) - f(\hat{u}_i^k)),$$

$$K\vartheta_{i+1}^k + \left(-2K - h^2\tau^{-\alpha} p_0^r + h^2 L\right)\vartheta_i^k + K\vartheta_{i-1}^k \le h^2\tau^{-\alpha}\sum_{j=0}^{k-1} p_{k-j}^{r}\vartheta_i^j. \tag{41}$$

To check stability using von Neumann method, let

$$\vartheta_i^k = \varkappa^k e^{I\omega ih}. \tag{42}$$

From (41) and (42), we have

$$K\varkappa^k e^{I\omega(i+1)h} + \left(-2K - h^2\tau^{-\alpha}p_0^r + h^2L\right)\varkappa^k e^{I\omega ih} + K\varkappa^k e^{I\omega(i-1)h} \le h^2\tau^{-\alpha}\sum_{j=0}^{k-1} p_{k-j}^r \varkappa^j e^{I\omega ih},$$

$$\varkappa^k \le \frac{h^2\tau^{-\alpha}}{-4K\,\sin^2\left(\frac{\omega h}{2}\right) - \left(h^2\tau^{-\alpha}p_0^r - h^2L\right)} \sum_{j=0}^{k-1} p_{k-j}^r \varkappa^j,$$

$$|\varkappa^k| \le \frac{|h^2\tau^{-\alpha}|}{|4K\,\sin^2\left(\frac{\omega h}{2}\right) + \left(h^2\tau^{-\alpha}p_0^r - h^2L\right)|} \sum_{j=0}^{k-1} |p_{k-j}^r||\varkappa^j|.$$

$4K\,\sin^2(\frac{\omega h}{2}) - h^2L$ can be made positive by choosing appropriate values of h, K, L, from which we can conclude that

$$\frac{1}{4K\,\sin^2\left(\frac{\omega h}{2}\right) - h^2L + h^2\tau^{-\alpha}p_0^r} \le \frac{1}{h^2\tau^{-\alpha}p_0^r}. \tag{43}$$

So we have

$$|\varkappa^k| \le \frac{1}{p_0^r}\sum_{j=0}^{k-1} |p_{k-j}^r||\varkappa^j|. \tag{44}$$

Now we prove that $|\varkappa^k| \le |\varkappa^0|$ for all k with the help of mathematical induction. For $k=1$, $|\varkappa^1| \le \frac{1}{|p_0^r|}|p_1^r||\varkappa^0|$. By property 1 of Lemma 1, we conclude that $|\varkappa^1| \le |\varkappa^0|$. Let us assume that $|\varkappa^j| \le |\varkappa^0|$ for $j = 1, 2, \ldots, k-1$. Now consider

$$|\varkappa^k| \le \frac{1}{p_0^r}\sum_{j=0}^{k-1} |p_{k-j}^r||\varkappa^j|$$

$$\le \frac{|\varkappa^0|}{p_0^r}\sum_{j=0}^{k-1} |p_{k-j}^r|.$$

By property 2 of Lemma 1, we see that

$$|\varkappa^k| \le |\varkappa^0|,$$

from which, we conclude that the perturbation term remains bounded by each progressing step in time direction and implies that the finite difference scheme is stable. □

Lemma 3. *The eigenvalues of the matrix A^k are given as $\lambda^i(A^k) = -4K\,\sin^2(\frac{i\pi}{N}) - h^2\tau^{-\alpha}p_0^r$, $i = 1, 2, \ldots, N-1$.*

For the proof of Lemma 3, refer to [43].

4.2 Convergence analysis

Theorem 4. *The finite difference scheme* (37) *has* $(r+1-\alpha)$ *order accuracy in temporal direction and* 2nd *order accuracy in spatial direction, i.e.,*

$$\|U^k - u^k\|_2 \le C(\tau^{r+1-\alpha}, h^2), \ \ k \ge r. \tag{45}$$

Proof. We use matrix analysis for proving the convergence of finite difference scheme (37) [43]. Let $E^k = U^k - u^k$, where U^k is the analytical solution and u^k is the numerical solution at kth time level where $k \geq r$. Subtracting (35) and (38) in their matrix form, we obtain

$$A^k(U^k - u^k) + h^2 I_{N-1}(f(U^k) - f(u^k)) = h^2\tau^{-\alpha}\sum_{j=0}^{k-1} p_{k-j}^r (U^j - u^j) + R^k,$$

$$\left(A^k + h^2 L I_{N-1}\right)E^k \leq h^2\tau^{-\alpha}\sum_{j=0}^{k-1} p_{k-j}^r E^j + R^k, \tag{46}$$

where $E^k = \left[E_1^k,\ E_2^k,\ \ldots,\ E_{N-1}^k\right]$, and $R^k = \left[R_1^k,\ R_2^k,\ \ldots,\ R_{N-1}^k\right]$. Taking inner product on both sides of (46) with E^k, we get

$$\langle A^k E^k, E^k\rangle + h^2 L\langle I_{N-1}E^k, E^k\rangle \leq h^2\tau^{-\alpha}\sum_{j=0}^{k-1} p_{k-j}^r \langle E^j, E^k\rangle + \langle R^k, E^k\rangle. \tag{47}$$

The property of the Rayleigh–Ritz ratio is given as [44, Theorem 4.2.2]

$$\lambda_{\min}(A) \leq \frac{\langle Ax, x\rangle}{\langle x, x\rangle} \leq \lambda_{\max}(A), \tag{48}$$

where A is any symmetric matrix and $0 \neq x \in R^{M-1}$. $\lambda_{\min}(A)$ is the minimum eigenvalue and $\lambda_{\max}(A)$ is the maximum eigenvalue of the matrix A. So we have

$$\begin{aligned}
\langle A^k E^k, E^k\rangle &\geq \lambda_{\min}(A^k)\|E^k\|^2,\\
\langle I_{N-1}E^k, E^k\rangle &\geq \lambda_{\min}(A^k)\|E^k\|^2 \geq \|E^k\|^2,\\
\langle E^j, E^k\rangle &\leq \|E^j\|\|E^k\|,\ \ \langle R^k, E^k\rangle \leq \|R^k\|\|E^k\|.
\end{aligned}$$

From (47), we have

$$(\lambda_{\min}(A^k) + h^2 L)\|E^k\| \leq h^2\tau^{-\alpha}\sum_{j=0}^{k-1} p_{k-j}^r \|E^j\| + \|R^k\|.$$

Using Lemma 3, we see that $\lambda_{\min}(A^k) = -h^2\tau^{-\alpha}p_0^r$. So we have

$$\begin{aligned}
\|E^k\| &\leq C\frac{1}{h^2 L - h^2\tau^{-\alpha}p_0^r}\sum_{j=0}^{k-1} h^2\tau^{-\alpha}p_{k-j}^r\|E^j\| + \|R^k\|\\
&\leq C\frac{1}{h^2 L - h^2\tau^{-\alpha}p_0^r}\exp\left(\frac{h^2\tau^{-\alpha}}{h^2 L - h^2\tau^{-\alpha}p_0^r}\sum_{j=0}^{k-1} p_{k-j}^r\right)\|R^k\|\\
&= C\frac{1}{h^2 L - h^2\tau^{-\alpha}p_0^r}\exp\left(\frac{p_0^r}{p_0^r - L\tau^{-\alpha}}\right)(\tau^{r+1-\alpha}, h^2)\\
&= C'(\tau^{r+1-\alpha}, h^2),\ \ k \geq r,
\end{aligned}$$

where $C' = \frac{C}{h^2 L - h^2\tau^{-\alpha}p_0^r}\exp\left(\frac{p_0^r}{p_0^r - L\tau^{-\alpha}}\right)$. The proof is completed. □

Table 6: Maximum absolute error and spatial convergence order for different h, α and fixed $\tau = 1/100$, $r = 4$ for Ex. 4.

α	N	Error	Order	*TIS*	*CPU*
	10	2.95120e-02		242	27.48
	20	7.66252E-03	1.945411810	242	40.75
0.2	40	1.91020E-03	2.004093662	242	42.79
	80	4.77212E-04	2.001025513	242	42.53
	160	1.19282E-04	2.000255526	242	40.46
	10	2.90044E-02		242	39.40
	20	7.53299E-03	1.944974253	242	42.75
0.4	40	1.87805E-03	2.003986013	242	84.96
	80	4.69188E-04	2.000997471	242	67.32
	160	1.17277E-04	2.000244102	242	76.12
	10	2.83264E-02		241	89.51
	20	7.35981E-03	1.944406392	241	93.77
0.6	40	1.83505E-03	2.003846132	241	99.32
	80	4.58459E-04	2.000957961	241	82.17
	160	1.14598E-04	2.000216307	241	61.39
	10	2.74297E-02		239	26.97
	20	7.13057E-03	1.943650436	239	27.40
0.8	40	1.77812E-03	2.003658330	239	38.51
	80	4.44257E-04	2.000893353	239	40.67
	160	1.11054E-04	2.000129927	239	43.80

Table 7: Maximum absolute error and spatial convergence order for different h, α and fixed $\tau = 1/100$, $r = 5$ for Ex. 4.

α	N	Error	Order	*TIS*	*CPU*
	10	2.95120E-02		242	127.31
	20	7.66252E-03	1.945411827	242	135.08
0.2	40	1.91020E-03	2.004093727	242	138.27
	80	4.77211E-04	2.001025773	242	134.98
	160	1.19282E-04	2.000256568	242	136.79
	10	2.90043E-02		242	133.95
	20	7.53299E-03	1.944974342	242	115.89
0.4	40	1.87805E-03	2.003986369	242	117.93
	80	4.69188E-04	2.000998896	242	118.78
	160	1.17276E-04	2.000249802	242	115.89
	10	2.83263E-02		241	161.76
	20	7.35981E-03	1.944406780	241	130.55
0.6	40	1.83505E-03	2.003847677	240	133.28
	80	4.58456E-04	2.000964136	240	130.52
	160	1.14594E-04	2.000241007	240	130.15
	10	2.74297E-02		238	153.92
	20	7.13056E-03	1.943651993	239	133.30
0.8	40	1.77811E-03	2.003664517	238	133.69
	80	4.44247E-04	2.000918090	238	130.46
	160	1.11044E-04	2.000228867	238	135.06

Table 8: Maximum absolute error and temporal convergence order for different $M = 1/\tau$, with $\alpha = 0.2$, fixed $h = 1/15,000$, $r = 4, 5$ for Ex. 4.

α	N	Error	Order	TIS
	10	5.17531E-06		28
	20	2.32392E-07	4.477014592	53
$r = 4$	40	1.01248E-08	4.520598741	102
	80	4.20470E-10	4.589740319	195
	160	1.42673E-11	4.881218922	381
	10	3.35065E-03		28
	20	5.23193E-05	6.000955227	53
$r = 5$	40	8.16878E-07	6.001078697	101
	80	1.41548E-08	5.850757996	194
	160	2.39396Ee-10	5.885746445	381

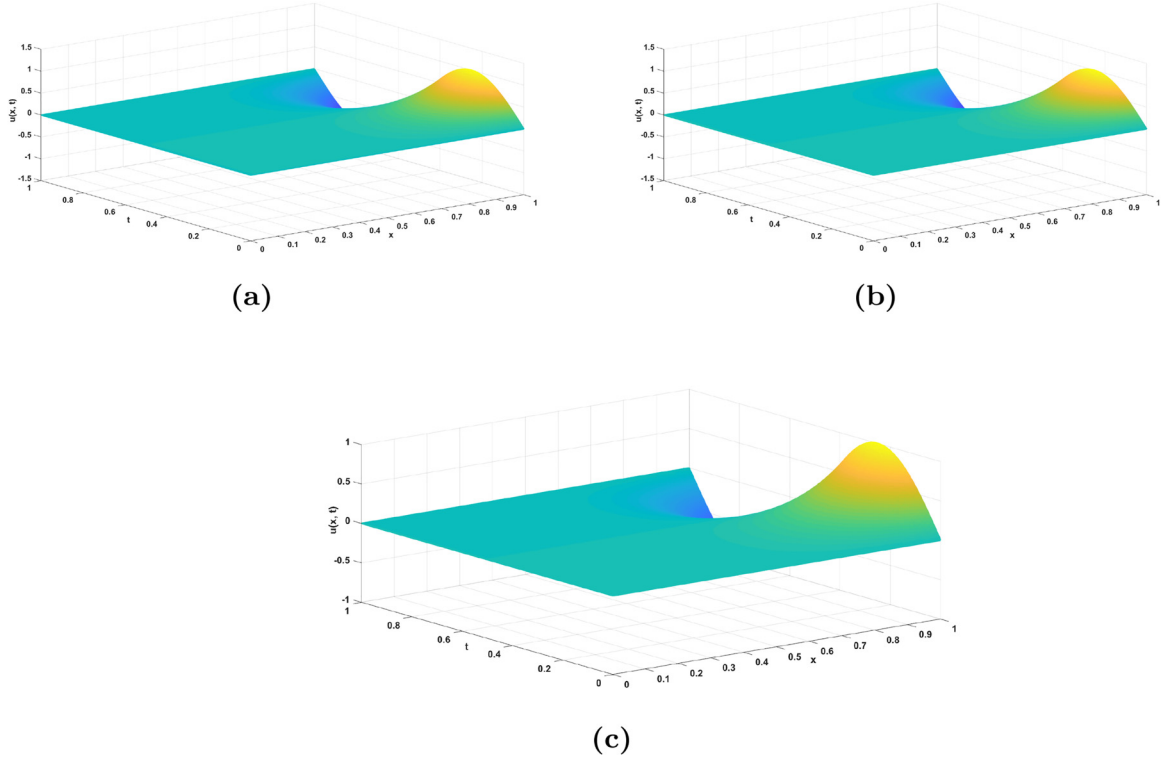

Figure 2: Numerical and analytical solutions when $\alpha = 0.5$ for Ex. 4. (a) Numerical solution when $r = 4$. (b) Numerical solution when $r = 5$. (c) Analytical solution.

4.3 Numerical experiments

Here, we discuss one numerical example for $r = 4$ and $r = 5$. Numerical experimentation is performed using (13) and (14).

Example 4. Consider the time fractional reaction–diffusion equation

$$ {}_0^{CP}D^{\gamma}_{\rho,\alpha,\omega}u(x,t) = u_{xx} + u(1-u^2) + g(x,t),\ \ 0 < x < 1,\ \ 0 < t < 1, $$

with initial and boundary conditions $u(x,0) = 0$, $u(0,t) = u(1,t) = 0$. The source term is $g(x,t) = 720\ \sin(2\pi x)t^{6-\alpha}E^{-\gamma}_{\rho,7-\alpha}(\omega t^{\rho}) + t^6\ \sin(2\pi x)(4\pi^2 - 1 + (t^6\ \sin(2\pi x))^2)$. The exact solution of (4) is $u(x,t) = t^6\ \sin(2\pi x)$. Here, the Lipschitz constant for the reaction term is 4. The maximum absolute error and convergence order are calculated with the help of the scheme (40) with tolerance 10^{-8}. The spatial convergence order for $r = 4, 5$ is shown in Tables 6 and 7 respectively for fixed $\tau = 1/100$, and the temporal convergence order is shown through Table 8 for fixed $h = 1/15,000$. Figure 2 gives a comparison between numerical solutions for $r = 4, 5$ and analytical solution. The obtained results validate the theoretically claimed convergence order.

5 Conclusions

An $(r + 1 - \alpha)$th-order accurate numerical scheme for approximating the Caputo–Prabhakar derivative of order $\alpha \in (0,1)$ is developed, using a time stepping interpolation polynomial of degree r. Later on, this developed scheme is combined with the central difference scheme for space discretization to solve a time fractional advection–diffusion equation and time fractional reaction–diffusion equation with nonlinear reaction term. The nonlinear reaction term is approximated using the Newton–Raphson iterative algorithm. Stability, solvability, and convergence analysis of the whole discretized scheme are studied rigorously. The delivered numerical results confirmed that analytically discussed convergence rates are achieved. Both the advection–diffusion equations and reaction–diffusion equations considered are assumed to have smooth solutions, however, Caputo–Prabhakar time fractional partial differential equations with nonsmooth solution will be the scope of our future study. The discussed high-order scheme can be applied to solve other linear and nonlinear fractional models involving the Caputo–Prabhakar derivative.

Acknowledgment: The first author acknowledges the financial support from the University Grants Commission, New Delhi, India under the SRF schemes.
Research ethics: Not applicable.
Informed consent: None declared.
Author contributions: All authors have accepted responsibility for the entire content of this manuscript and approved its submission.
Competing interests: The authors state no conflict of interest.
Research funding: None declared.
Data availability: Not applicable.

References

[1] J. F. Douglas, “Some applications of fractional calculus to polymer science,” *Adv. Chem. Phys.*, vol. 102, pp. 121—192, 1997.
[2] E. A. Gonzalez and I. Petr’avs, “Advances in fractional calculus: control and signal processing applications,” in *Proceedings of the 2015 16th International Carpathian Control Conference (ICCC)*, IEEE, 2015, pp. 147—152.
[3] A. K. Shukla, R. K. Pandey, and R. B. Pachori, “A fractional filter based efficient algorithm for retinal blood vessel segmentation,” *Biomed. Signal Process. Control*, vol. 59, 2020, Art. no. 101883.
[4] Q. Yang, D. Chen, T. Zhao, and Y. Q. Chen, “Fractional calculus in image processing: a review,” *Fract. calc. Appl. Anal.*, vol. 19, no. 5, pp. 1222—1249, 2016.
[5] R. Hilfer, *Applications of Fractional Calculus in Physics*, Singapore, World Scientific, 2000.
[6] H. G. Sun, Y. Zhang, D. Baleanu, W. Chen, and Y. Q. Chen, “A new collection of real world applications of fractional calculus in science and engineering,” *Commun. Nonlinear Sci. Numer. Simul.*, vol. 64, pp. 213—231, 2018.
[7] J. Sabatier, O. P. Agrawal, and J. A. Tenreiro Machado, *Advances in Fractional Calculus*, vol. 4, Netherland, Springer, 2007.
[8] L. Debnath, “Recent applications of fractional calculus to science and engineering,” *Int. J. Math. Math. Sci.*, vol. 2003, no. 54, pp. 3413—3442, 2003.
[9] A. Kilbas, Anatoli, H. M. Srivastava, and J. J. Trujillo, *Theory and Applications of Fractional Differential Equations*, vol. 204, Netherland, Elsevier, 2006.
[10] C. Li and M. Cai, *Theory and Numerical Approximations of Fractional Integrals and Derivatives*, Philadelphia, SIAM, 2019.
[11] C. Li and F. Zeng, *Numerical Methods for Fractional Calculus*, UK, Chapman and Hall/CRC, 2015.

[12] D. Baleanu, K. Diethelm, E. Scalas, and J. J. Trujillo, *Fractional Calculus: Models and Numerical Methods*, vol. 3, Singapore, World Scientific, 2012.
[13] T. R. Prabhakar, *et al*, *A Singular Integral Equation with a Generalized Mittag—Leffler Function in the Kernel*, Yokohama, Yokohama City University, 1971.
[14] R. Garra and R. Garrappa, "The Prabhakar or three parameter Mittag—Leffler function: theory and application," *Commun. Nonlinear Sci. Numer. Simul.*, vol. 56, pp. 314—329, 2018.
[15] F. Mainardi and R. Garrappa, "On complete monotonicity of the Prabhakar function and non-debye relaxation in dielectrics," *J. Comput. Phys.*, vol. 293, pp. 70—80, 2015.
[16] H. M. Srivastava, A. Fernandez, and D. Baleanu, "Some new fractional calculus connections between Mittag—Leffler functions," *Mathematics*, vol. 7, no. 6, p. 485, 2019.
[17] R. Garrappa, "Numerical evaluation of two and three parameter Mittag—Leffler functions," *SIAM J. Numer. Anal.*, vol. 53, no. 3, pp. 1350—1369, 2015.
[18] R. Garrappa, *The Mittag—Leffler Function, MATLAB Central File Exchange*, vol. 201, 2014, p. 48154.
[19] A. Giusti, *et al*., "A practical guide to Prabhakar fractional calculus," *Fract. calc. Appl. Anal.*, vol. 23, no. 1, pp. 9—54, 2020.
[20] A. Giusti, "General fractional calculus and Prabhakar theory," *Commun. Nonlinear Sci. Numer. Simul.*, vol. 83, pp. 105—114, 2020.
[21] A. Giusti and I. Colombaro, "Prabhakar-like fractional viscoelasticity," *Commun. Nonlinear Sci. Numer. Simul.*, vol. 56, pp. 138—143, 2018.
[22] R. Garrappa and G. Maione, "Fractional Prabhakar derivative and applications in anomalous dielectrics: a numerical approach," in *In Theory and Applications of Non Integer Order Systems*, Springer, 2017, pp. 429—439.
[23] D. Zhao and H. G. Sun, "Anomalous relaxation model based on the fractional derivative with a Prabhakar-like kernel," *Z. Angew. Math. Phys.*, vol. 70, no. 2, pp. 1—8, 2019.
[24] D. Abbaszadeh, M. Tavassoli Kajani, M. Momeni, M. Zahraei, and M. Maleki, "Solving fractional Fredholm integro-differential equations using Legendre wavelets," *Appl. Numer. Math.*, vol. 166, pp. 168—185, 2021.
[25] H. R. Marasi and M. H. Derakhshan, "Haar wavelet collocation method for variable order fractional integro-differential equations with stability analysis," *Comput. Appl. Math.*, vol. 41, no. 3, pp. 1—19, 2022.
[26] B. Bagharzadehtvasani, A. Hosein Refahi Sheikhani, and H. Aminikhah, "A numerical scheme for solving variable order Caputo-Prabhakar fractional integro differential equation," *Int. J. Nonlinear Anal. Appl.*, vol. 13, no. 1, pp. 467—484, 2022.
[27] M. H. Derakhshan and A. Ansari, "Numerical approximation to Prabhakar fractional Sturm-Liouville problem," *Comput. Appl. Math.*, vol. 38, no. 2, pp. 1—20, 2019.
[28] S. Eshaghi, A. Ansari, R. K. Ghaziani, and M. Ahmadi Darani, "Fractional Black—Scholes model with regularized prabhakar derivative," *Publ. Inst. Math.*, vol. 102, no. 116, pp. 121—132, 2017.
[29] S. Eshaghi, R. K. Ghaziani, and A. Ansari, "Stability and dynamics of neutral and integro-differential regularized Prabhakar fractional differential systems," *Comput. Appl. Math.*, vol. 39, no. 4, pp. 1—21, 2020.
[30] M. H. Derakhshan and A. Aminataei, "Comparison of homotopy perturbation transform method and fractional Adams—Bashforth method for the Caputo—Prabhakar nonlinear fractional differential equations," *Iran. J. Numer. Anal. Optim.*, vol. 10, no. 2, pp. 63—85, 2020.
[31] R. Garrappa and E. Kaslik, "Stability of fractional-order systems with Prabhakar derivatives," *Nonlinear Dyn.*, vol. 102, no. 1, pp. 567—578, 2020.
[32] D. Singh, F. Sultana, and R. K. Pandey, "Approximation of Caputo—Prabhakar derivative with application in solving time fractional advection—diffusion equation," *Int. J. Numer. Methods Fluids*, vol. 94, no. 7, pp. 896—919, 2022.
[33] A. Mohebbi and M. Abbaszadeh, "Compact finite difference scheme for the solution of time fractional advection—dispersion equation," *Numer. Algorithms*, vol. 63, no. 3, pp. 431—452, 2013.
[34] J. Cao, C. Li, and Y. Q. Chen, "High-order approximation to Caputo derivatives and Caputo-type advection—diffusion equations (ii)," *Fract. calc. Appl. Anal.*, vol. 18, no. 3, pp. 735—761, 2015.
[35] J. Zhang, X. Zhang, and B. Yang, "An approximation scheme for the time fractional convection diffusion equation," *Appl. Math. Comput.*, vol. 335, pp. 305—312, 2018.
[36] S. Yadav, R. K. Pandey, A. K. Shukla, and K. Kumar, "High-order approximation for generalized fractional derivative and its application," *Int. J. Numer. Methods Heat Fluid Flow*, vol. 29, no. 9, pp. 3515—3534, 2019.
[37] S. Yadav, R. K. Pandey, and A. K. Shukla, "Numerical approximations of Atangana Baleanu Caputo derivative and its application," *Chaos, Solitons Fractals*, vol. 118, pp. 58—64, 2019.
[38] X. Hu, F. Liu, I. Turner, and V. Anh, "An implicit numerical method of a new time distributed-order and two-sided space-fractional advection—dispersion equation," *Numer. Algorithms*, vol. 72, no. 2, pp. 393—407, 2016.
[39] H. Li, J. Cao, and C. Li, "High-order approximation to Caputo derivatives and Caputo-type advection— diffusion equations (iii)," *J. Comput. Appl. Math.*, vol. 299, pp. 159—175, 2016.
[40] D. Singh, F. Sultana, R. K. Pandey, and A. Atangana, "A comparative study of three numerical schemes for solving Atangana—Baleanu fractional integro-differential equation defined in Caputo sense," *Eng. Comput.*, vol. 38, pp. 149—168, 2022.
[41] G. D. Smith, *Numerical Solution of Partial Differential Equations: Finite Difference Methods*, UK, Oxford University Press, 1985.
[42] J. M. Varah, "A lower bound for the smallest singular value of a matrix," *Linear Algebra Appl.*, vol. 11, no. 1, pp. 3—5, 1975.

[43] D. Singh, R. K. Pandey, and S. Kumari, "A fourth order accurate numerical method for non-linear time fractional reaction—diffusion equation on a bounded domain," *Phys. D*, vol. 449, 2023, Art. no. 133742.
[44] A. Quarteroni and A. Valli, *Numerical Approximation of Partial Differential Equations*, Italy, Springer Science & Business Media, 2008, p. 23.